RAFSS 2014 REGIONAL ANNUAL FUNDAMENTAL SCIENCE SYMPOSIUM 2014
Ibnu Sina Institute for Fundamental Science Studies

Immobilization of Metalloporphyrin on Functionalized SBA-15 Nanoporous Silica

Nurafiqah Saadon[a], Salasiah Endud[b,c,*], Mohd Bakri Bakar[2]

[a] *Novel Materials Research Group Nanotechnology Research Alliance, Universiti Teknologi Malaysia, 81310 UTM Johor Bahru, Johor, Malaysia .*
[b] *Department of Chemistry, Faculty of Science, Universiti Teknologi Malaysia, 81310 UTM Johor Bahru, Johor, Malaysia.*

**Corresponding Author: salasiah@kimia.fs.utm.my*

Article history :
Received 1 February 2013
Revised 20 July 2013,
Accepted 25 July 2013,
Available online 15 August 2013

GRAPHICAL ABSTRACT

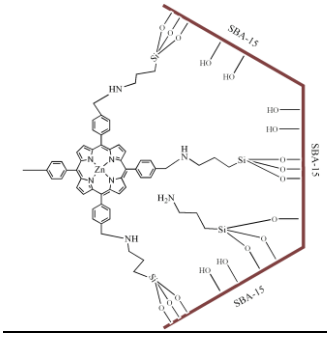

ABSTRACT

SBA-15 nanoporous silica were prepared cooperation assembly of tetraethylorthosilicate precursor in the presence of poly (ethylene glycol)–block- poly (propylene glycol)–block- poly (ethylene glycol) copolymer surfactant and functionalized with (3-aminopropyl) triethoxysilane (APTES) via sol-gel reaction to obtain APTES-SBA-15. Tetra-(p-chlorophenyl) porphyrin (TClPP) was synthesized using slightly modified Alder- Longo method and zinc(II) was inserted into the TClPP using zinc acetate as source of zinc. The existance of zinc metal in porphyrin was confirmed by the appearance of Soret band and Q band in UV- vis spectra. Zn(II)-TClPP was also characterized using FTIR and NMR spectroscopy .With the aid of amino functionalized on surface of SBA-15, it can be used as support for immobilization of metalloporphyrin producing APTES-SBA-15-Zn(II)-TClPP that can used as heterogenous catalysis in various reactions. The formation of this material was confirmed by characterization by using FTIR spectroscopy, XRD and BET adsorption.

Keywords: nanoporous silica, metalloporphyrins, APTES

| 1823-626X | http://dx.doi.org/xx.xxx/xxx.xxx.xxx |

1. INTRODUCTION

Porphyrins are any group of compounds containing porphine structure to which a variety of side chains are attached. They consist of an important class of molecules that work in nature in many different ways. Many of the synthetic porphyrins are the basic structure of biological porphyrins which are the active sites of numerous proteins.

Metalloporphyrins is the porphyrins that consists metal in the centre of the porphyrins ring. Natural metalloporphyrins species have been found in chlorophyll and heme. Metal complexes of tetrapyrollic macrocyles play an essential role to life on earth due to their implications in many enzymatic systems [1]. Hence, synthetic analogues featuring the characteristic porphyrins macromolecule have been expected to have a great application potential. Synthetic porphyrins and metalloporphyrins have been reported to have broad applications in biological catalyst and electron transfer systems. Moreover, relative easy syntheses of porphyrins at moderate cost and have the possibilities in creating variety of structural modifications offer almost unlimited prospect to molecular design [2].

Metalloporphyrin always associated with iron-porphyrin but there are also widely researches on other metals binded to porphyrin. Various types of metals such Co, Zn, Cu, Mn, Ru and many more can be inserted into the porphyrin cavity by using various metal salts.There have been many research on application of metalloporphyrin in this field such as act mimicking enzyme, ion receptor [3], pesticide photodegradation [4] and many more. The well known metalloporhyrin for mimicking of oxygenation function of enzyme, cytochrome P450 have faced major problem- the easy formation of μ-oxo dimers from several of porphyrin-matallocomplexes in mimicking such transformation with synthetic receptor. Cytochrome P450 mimicking solved the major problem of catalyst inactivation by introduction of electronegative substitution (electron withdrawing group at meso-phenyl or β-pyrrole position) which prevent undesired reduction of catalytic activity [5].

However, metalloporphyrins used as homogeneous catalyst system that have several disadvantages such as their oxidative self-destruction in oxidizing media and decomposition of catalyst during reactions and difficulty of recovery at the end of reaction for reuse [6]. Homogenous catalysts are difficult to separate the catalyst and the product, thus increase the cost of production.

One of the suggested ways to overcome these problems is to immobilize the porphyrin on the solid matrix such as alumina, silica and clays. Some advantages such as increasing catalytic activity, stability and reusability. In addition, heterogenization of metalloporphyrin will prevent the formation of inactive dimers [7].

In this study, mesoporous silica sieves is chosen to be used as support material due to their large pores size, so high molecular mass molecules can permit an efficient diffusion of products and reagents. These types of materials are structurally stable, environmentally acceptable and chemically more resistance to organic solvent more than organic support. Mesoporous material are also high controllable and mono disperse nature of large accessible pore size, high surface plus periodic nano- scale pore spacing that make they are suitable for application as heterogeneous catalyst [8]. Deposition on silica support has positively influence the stability of metalloporphyrin species.

Among these ordered mesoporous silica materials, SBA-15 is a mesoporous material that is synthesized by triblock copolymer surfactant as template under acidic conditions, suppress other materials such as M41S family due to its larger pore size (up to 30nm) and better stability. SBA-15 shows higher thermal and hydrothermal stability, significantly larger unit cell size, wider and ordered pores, high structural regularity, well defined morphologies as well as ticker pore size compared to MCM-41and MCM-48. Larger pore enable immobilized the larger molecules, which is cannot be applied in the small pores size. These characteristic make them suitable for practical applications in materials science and catalysis.

2. EXPERIMENTS

2.1 Synthesis of APTES-SBA-15

SBA-15 was synthesized using Zhao method [9]. Similar to other methods, 4.0 g of poly (ethylene glycol)–block- poly (propylene glycol)–block- poly (ethylene glycol) copolymer was dissolved in 30 g of water and 120 g of 2M of hydrochloric acid (HCl) solution while stirring at 35 °C. After that the copolymer was completely dissolved, 8.5 g of tetraethyl orthosilicate (TEOS) was added into the mixture and keep stirring for 20 hours. The mixture then was aged in the oven at 80 °C overnight without stirring. The product was recovered, washed and dried. The calcinations process was performed at 1°C/ min up to 550°C for 6 hours. The pure silica SBA-15 then functionalized with (3-aminopropyl) triethoxysilane (APTES) with formula- 0.01 mol of liquid silane derivatives for 1g of support [10]. Calcined SBA-15, APTES and 100mL of toluene were refluxed at 85°C for 24 hours. The resulting mixture was allowed to cool and washed repetitively using toluene and diethylether. The NH-SBA-15 was dried at ambient temperature in the desiccator.

2.2 Synthesis of Zinc (II) Tetra-(p-chlorophenyl) porphyrin (ZnTClPP)

Tetrakis (p- chlorophenyl) porphyrin was synthesized by slightly modified Alder-Longo method [6]. The synthesizing process was started with refluxing 100 mL of propanoic acid, freshly prepared pyrrole (0.05 mol) and 4-chlorobenzaldehyde (0.05 mol) for 30 minutes. The colorless solution will turn into dark purple solution when the mixture was boiled. After filtered and washed with cold methonal and hot water to give violet solid of tetrakis (p-chlorophenyl) porphyrin. Zinc(II) - tetra-(p-chlorophenyl) porphyrin (Zn-TClPP) was prepared by refluxing TCP (1 mmol) and Zinc Acetate (1 mmol) in dichloromethane (DCM) at 100 °C in oil bath for 1 hour. After that, the solution was filter while still hot, washes with water and dried at room temperature.

2.3 Immobilization of ZnTClPP on APTES functionalized SBA-15

Preparation of the material was carried out using method from reported paper [6]. The Zn(II)- tetra- (p-chlorophenyl) porphyrin was added to a suspension of NH-SBA-15 in dry toluene and triethylamine. The mixture was refluxed at 110°C in oil bath for 24 hours. The solid product then was filtered and washed with toluene, DCM and distilled water. The NH-SBA-15-ZnP was dried in the oven and grounded into fine powder.

2.4 Characterizations

The material was characterized using spectroscopic and physical methods including FTIR spectroscopy (Perkin Elmer Series 1600 Spectrophotometer), UV-Vis spectroscopy (Perkin Elmer Lambda 900 UV-VIS-NIR spectrometer), ^{1}H NMR Spectroscopy (Bruker DPX-400 MHz NMR spectrophotometer), XRD analysis (X-Ray Diffractiometer model Bruker D8) and Diffuse Reflectance UV-Vis spectroscopy ().

3. RESULTS AND DISCUSSION

3.1 Characterization of TClPP and ZnTClPP

The ^{1}H NMR spectra of free base porphyrin gives three characteristic proton resonance: a) β- pyrrole protons, b) imino protons, and c) meso-aryl protons [1]. From the ^{1}H NMR spectrum of TClPP in deuterium chloroform ($CDCl_3$), the singlet highly shielded peak at -2.84ppm indicated the inner N-H of the porphyrin. This is due to the rapidly exchanging N-H proton at the centre of porphyrin ligand in the core of molecule. However, this peak disappeared upon metallated Zn(II) porphyrin because H atoms are replaced by Zn metal ion. This indicated that the zinc has successfully incorporated into the core of porhyrin. The β- protons in porphine skeleton were strongly deshielded by anisotropic effect of substituent ring current. Hence, singlet peak resonated at 8.87ppm was attributed to the eight proton in the basic core of porphyrin (Table 1).

Figure 1 present the FTIR spectra of TClPP and ZnTClPP. The results show the presence of N-H stretching vibration of pyrrole at 3445 cm^{-1} as well as N-H in planarity absorption at 965 cm^{-1}. The zinc metal insertion into porphyrin ring was confirmed by the disappearance of N-H peaks in Zn-TClPP spectrum because the lost of H atom at secondary amine (=N-H) when coordinated with

zinc(II) ions .Therefore, there are no N-H vibration appeared. The vibration at 3322 cm^{-1} and 2921 cm^{-1} wavelength represent C-H (sp^2) stretching of macromolecule and C-H (sp^2) stretching of phenyl group respectively. C=C stretching of aromatic rings from phenyl presence at 1635 cm^{-1} and 1394 cm^{-1} for TClPP while for ZnTClPP they are appeared at 1637 cm^{-1} and 1338 cm^{-1} . The C-Cl stretching vibration is seen at both spectra at 800 cm^{-1} and 797 cm^{-1}.

Table 1 ^{1}H NMR data of TClPP and Zn-TClPP

Porphyrins	β- pyrrole	Imino protons	Meso-aryl protons
TClPP	8.87 ppm (s,8H)	-2.84 ppm (s)	8.15 ppm (d,8H,H_o), 7.77 ppm (d,8H,H_m)
Zn- TClPP	8.96 ppm (s,8H)	-	8.16 ppm (d,8 H_o) 7.76 ppm (d,8H, H_m)

***** The nature of splitting pattern (s: Singlet, d: doublet, t: triplet, m: multiplet).
* Their location in porphyrins respectively are given on parenthesis (o: ortho, p: para, m: meta).

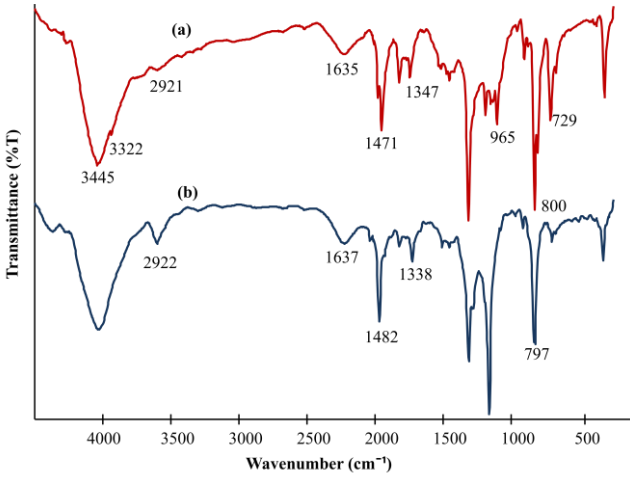

Figure 1 FTIR spectra of TClPP and ZnTClPP

The Figure 2 shows the UV- Vis spectra of TClPP and Zn-TClPP. The UV-Vis spectrum of TClPP in DCM showed the etio type absorption spectrum. The maximum absorbance presence at 427 nm which was assigned as Soret band and four small bands at 523 nm, 557 nm, 600 nm and 654 nm were assigned as Q bands. Both Soret and Q bands are 'fingerprint' of porphyrin absorption spectra After metallation of zinc process, there are only two bands, at 557 nm and 600 nm. The Soret band of Zn-TClPP was found at 430 nm.

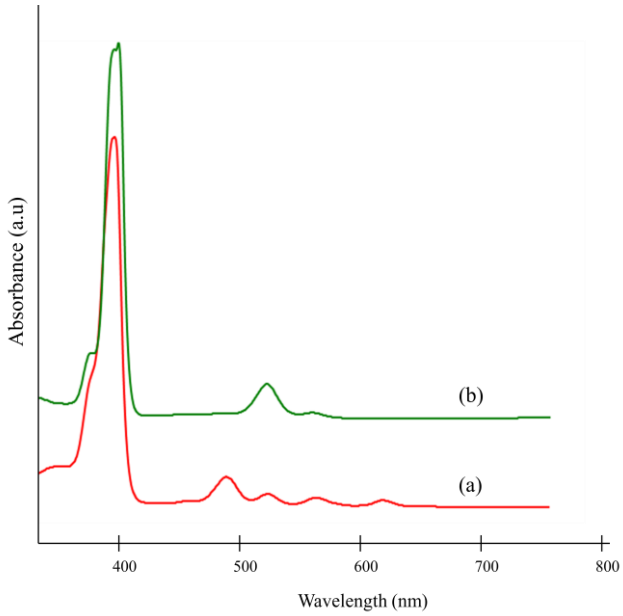

Figure 2 UV-Vis spectra of TClPP and ZnTClPP

Elemental analysis of TClPP and ZnTClPP are also characterized by using Maldi-Tof-Tof MS/MS and data is accumulated in Table 2.

Table 2 Comparison of molecular weight of TClPP and ZnTClPP

Porphyrin	Molecular structure	Calculated molecular weight (g/mol)	Maldi-Tof analysis
TClPP	$C_{44}H_{26}C_{l4}N_4$	752.52	752.04
Zn-TClPP	$C_{44}H_{24}C_{l4}N_4Zn$	815.89	815.94

3.2 Characterization of APTES-SBA-15-ZnTClPP

The FTIR spectra of SBA-15, NH-SBA-15 and NH-SBA-15-ZnP are shown in Figure 3. The broad peak around 3400 cm^{-1} in all three spectra indicated that Si-OH stretching which SBA-15 compared to NH-SBA-15 and NH-SBA-15-ZnP because most of the Si atom have been reacted and form bond to N-H group of APTES. Added by the presence of C-H and N-H stretching vibration of on the surface of mesoporous SBA-15 can be seen at 2938 cm^{-1} and 1562 cm^{-1} for NH-SBA-15 as well as at 2933 cm^{-1} and 1592 cm^{-1} for NH-SBA-15 ZnP. Asymmetric stretching vibration of Si-O-Si appeared at all spectra at 1086 cm^{-1} SBA-15, 1083 cm^{-1} for NH-SBA-15 and 1078 cm^{-1} for NH-SBA-15-ZnP. Another band at 1385 cm^{-1} appeared at both NH-SBA-15 and NH-SBA-15 ZnP was representing C-N stretching of primay amides.

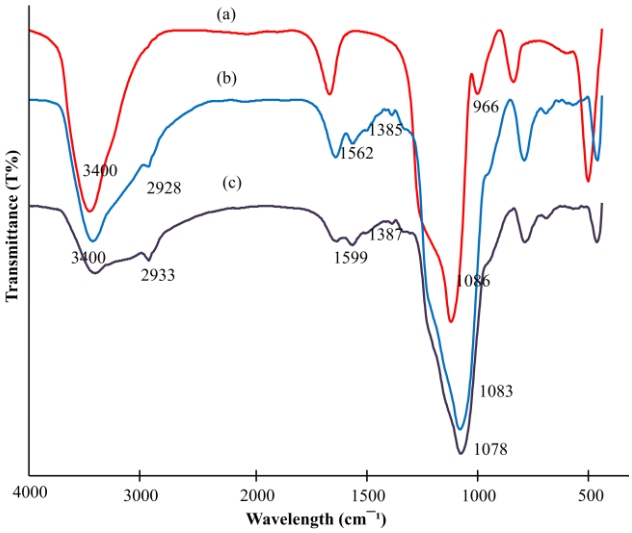

Figure 3 FTIR spectra of a) SBA-15 b) NH-SBA-15 c) NH-SBA-15 ZnP

Figure 4 shows the XRD pattern of the pure SBA-15 and NH-SBA-15 ZnP. The result of pure SBA-15 showed three well-resolved diffraction peaks with intense peak at 2θ of 0.9° to 1.0° and two small peaks at 1.2° to 2.0°. These peaks could be indexed to (1 0 0), (1 1 0) and (2 0 0) planes which correspond to mesostructure of hexagonal space with group symmetry of *p6mm*. The XRD pattern of NH-SBA-15 show similar pattern as SBA-15 indicated that the mesoporous hexagonal structure of NH-SBA-15 ZnP is still retained and maintained even though after functionalization of APTES and immobilization of ZnTClPP into SBA-15. The hexagonal mesoporous structure of SBA-15 does not collapsed hence, confirmed that SBA-15 has thermal stability.

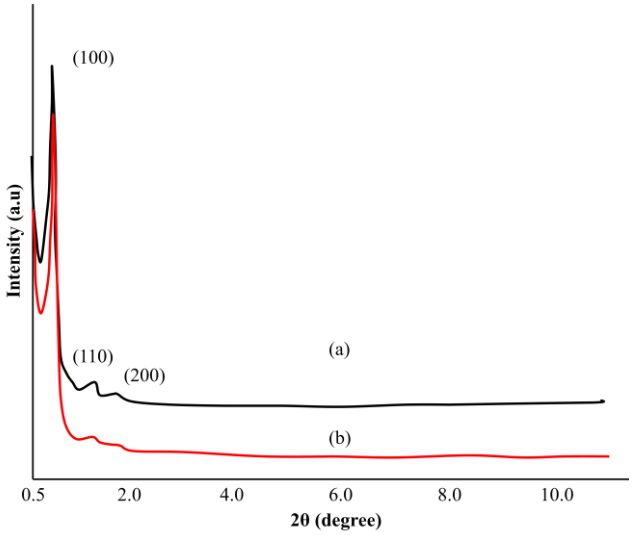

Figure 4 XRD patterns of (a) SBA-15 and (b) NH-SBA-15 Zn-P

The N_2 adsorption- desorption isotherm of pure SBA-15 and NH-SBA-15 were found to be type IV curve which is typical for mesoporous materials with well- defined capillary condensation step and uniform mesoporous materials. The characteristic features of the type IV isothermis it hysteresis loop. Based on the IUPAC classification, isotherm of SBA-15 has the characteristic of hysteresis loop type H2. This H2 type associated with capillary condensation in 'ink bottle' pores which having narrow neck and wide body. The surface area BET analysis of SBA-15 and NH-SBA-15 ZnP are 851 m^2g^{-1} and 242 m^2g^{-1} respectively. The decreased in surface area of SBA-15 could because of the immobilization of ZnClPP, result less of surface area. The reduction in pore diameter of NH-SBA-15 ZnP compared to SBA-15 could be also due to the 'clog' by ZnTClPP complex moiety.

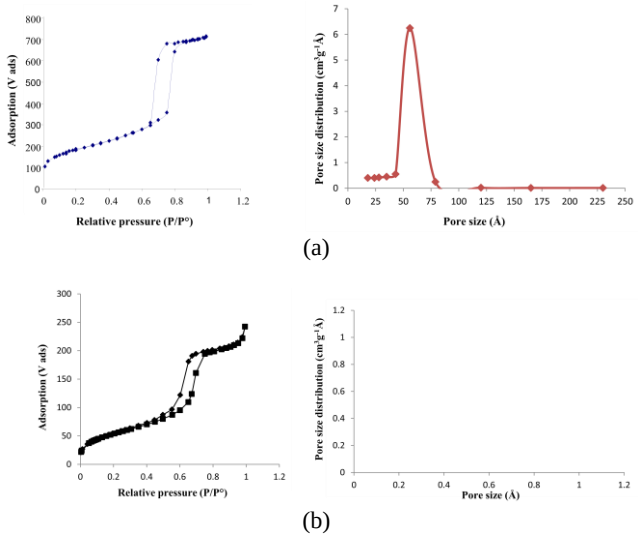

Figure 5 N_2 adsorption- desorption isotherm and pore size distribution curve of a) SBA-15 b) NH-SBA-15 ZnP

The DR-UV-Vis spectra of pure SBA-15 and NH-SBA-15 ZnP are shown in Figure 6. Compared to pure SBA-15 spectrum, the typical intense Soret band of porphyrin appeared at 428nm in the NH-SBA-15 ZnP spectrum. There are two more peaks that called Q band detected in NH-SBA-15 ZnP spectrum at 563nm and 608nm.The bands were red-shifted to lower energy compared to ZnTClPP possibly due the distortion of the porphyrin ring during the immobilization of metalloporphyrin into SBA-15. The DR-UV-Vis spectra of NH-SBA-15 ZnP seem to be similar to that ZnClTPP without any significant differences show that the porphryin structural attached to mesoporous silica neither destruct nor collapsed.

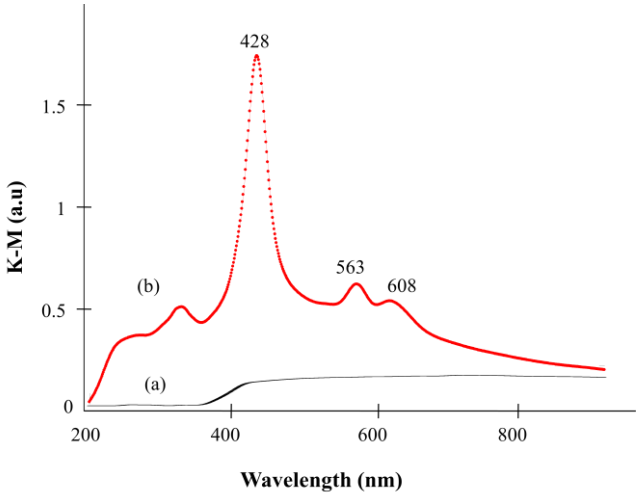

Figure 6 DR-UV-Vis spectra of (a) SBA-15 and (b) NH-SBA-15 Zn-P

4. CONCLUSION

The ZnTClPP was successfully synthesized, proved by the spectroscopic evidences that obtained by using modified Alder-Longo method and insertion of zinc (II) using zinc acetate as metal precursor. After the immobilization of ZnTClPP into NH-SBA-15 the surface area do decrease from 851m^2g^{-1} to 242 m^2g^{-1} but maintained the mesoporous hexagonal structure and pore shape of SBA-15.

ACKNOWLEDGEMENT

This research was supported by …., myMaster scholarship (Nurafiqah Saadon) from Ministry of Education.

REFERENCES

[1] Bajju, D.G.; Kundan, S.; Kapahi, A.; Gupta, D. J. Chem 2013 (2013). 1-14.
[2] Slota, R.; Broda, M.A.; Dyrda, G.; Ejsmont, K.; Mele, Giuseppe. Molecules (2011). 16. 9957-9971.
[3] Bao, X.; Zhang, H.; Zhang, Z.; Wu, L.; Li, Z. Inorg. Chem. Comm. 10 (2009). 728-730
[4] Silva, M.; Azenha, M.E.; Pereira, M.M.; Burrows, H.D.; Sarakha, M.; Forano, C.; Ribeiro, M.F.; Fernandes, A. Appl. Catal. B: Envi. 100 (2010). 1-9
[5] Pulkkinen, J.; Zachar, P.; Borek, V.A.; Laatikainen, R.; Kral, V. J. Mol. Catal. A: Chem. 219. (2004). 21-27
[6] Adam, F.; Ooi, W.T. Appl. Sci. A: Gen. 445-446. (2012). 252-260
[7] Serwika, E.M.; Poltowicz, J.; Bahranowski, K.; Olenjniczak, Z.; Jones, W. Appl. Catal. A: Gen. 275 (2009). 9-14.
[8] Zhang, H.; Sun, Y.; Ye, K.; Zhang, P.; Wang, Y. J. Mat. Chem.15 (2005). 3181-3186
[9] Zhao, D.; Feng, J.; Huo, Q.; Melosh, N.; Fredrickson, G.H.; Chmelka, B.F.; Stucky, G.D. Sci. 279 (1998) 548–552
[10] Dragoi, B.; Dumitriu, E. Acta. Chim. Slov. 55 (2008). 277-285